Massive MIMO in Mobile Networks: Self-Calibration with Channel Estimation Error

De Mi
University of Surrey
d.mi@surrey.ac.uk

Hongzhi Chen
University of Surrey
hongzhi.chen@surrey.ac.uk

Zhen Gao
Beijing Institute of Technology
gaozhen16@bit.edu.cn

Lei Zhang
University of Glasgow
lei.zhang@glasgow.ac.uk

Pei Xiao
University of Surrey
p.xiao@surrey.ac.uk

ABSTRACT

Time-division-duplexing (TDD) massive multiple-input multiple-output (MIMO) systems will play a crucial role in the deployment of emerging mobile networks in 5G and beyond. Such systems heavily rely on the reciprocity-based channel estimation for its scalability. However, the imperfect channel reciprocity, mainly caused by radio-frequency mismatches among the base station antennas, can contaminate the estimate of the effective channel response thus become a performance-limiting factor. In practice, self-calibration schemes are often applied to compensate for this type of imperfections. This work investigates two self-calibration schemes, namely relative calibration and inverse calibration. Considering a TDD massive multi-user MIMO system in the presence of both channel reciprocity error and imperfect channel estimation, we derive closed-form expressions for the receive mean-square error and provide an in-depth comparative analysis of the post-equalisation performance of two calibration schemes. The proposed analytical results are verified via Monte-Carlo simulations.

CCS CONCEPTS

• **Networks** → **Wireless access networks**.

KEYWORDS

massive MIMO, channel reciprocity, self calibration, channel estimation

ACM Reference Format:
De Mi, Hongzhi Chen, Zhen Gao, Lei Zhang, and Pei Xiao. 2020. Massive MIMO in Mobile Networks: Self-Calibration with Channel Estimation Error. In *ACM MobiArch 2020 The 15th Workshop on Mobility in the Evolving Internet Architecture (MobiArch'20), September 21, 2020, London, United Kingdom.* ACM, New York, NY, USA, 6 pages. https://doi.org/10.1145/3411043.3412507

MobiArch'20, September 21, 2020, London, United Kingdom

ACM ISBN 978-1-4503-8081-2/20/09…$15.00
https://doi.org/10.1145/3411043.3412507

1 INTRODUCTION

The explosive growth of connected devices and the growing number of broadband subscribers have led to unprecedented growth in traffic demand of the current mobile internet. To this effect, a promising multi-user (MU) massive MIMO (multiple-input-multiple-output) technology has evolved in the 5th generation (5G) mobile networks [1], operating by a large scale base station (BS) antennas, typically in the order of hundreds or perhaps thousands [2–4]. One key advantage of massive MIMO over the conventional MU-MIMO in the future mobile network deployment, is that simple linear processing algorithms perform very well at both uplink (UL) and downlink (DL), due to the significant imparity between the number of service-antennas at the BS and that of the user terminals (UTs) [5, 6]. Prior investigations in the context of the massive MIMO downlinks [7, 8] show that typical linear precoding schemes, such as maximum ratio transmission (MRT) and zero-forcing (ZF), can achieve a spectral efficiency close to the optimal non-linear precoding techniques, but with a relatively low computational complexity. However, these channel-aware linear precoding schemes are susceptible to the accuracy of the channel state information (CSI).

One of the main challenges in building up mobile networks with massive MIMO is the CSI acquisition at the BS, which significantly increases the signalling overhead, posing a practical hindrance in performance, in terms of both spectral and energy efficiency. Considering that in a time-division-duplexing (TDD) system, where the UL and DL channels are reciprocal, exploiting channel reciprocity, therefore, enables implicit DL channel estimation. Most prior investigations assume perfect channel reciprocity in TDD massive MIMO systems [2, 7, 9]. However, such assumption is over-strong in practical scenarios, due to amplitude and phase mismatches between the UL and the DL as well as radio-frequency (RF) mismatch between transmit (Tx) and receive (Rx) RF frontends of the BS antennas [10, 11]. These mismatches contaminate the estimate of the effective channel response, causing a significant degradation in the performance of linear precoding schemes in the massive MIMO system. Our prior work, [12], thoroughly investigated the performance degradation for the MRT and ZF precoders under imperfect channel estimation. The results in [12] show that both MRT and ZF are severely affected by the compound effect of the reciprocity and estimation errors.

In practice, calibration schemes are often used in a TDD MIMO system to restore the reciprocity of its effective channel response.

Two prevalent schemes have been offered in MIMO systems: over-the-air calibration [13] and self-calibration [14]. The former requires an exchange of pilots between UTs and the BS during the calibration phase. Due to the large number of the required pilots, which is proportional to the number of the BS antennas, it may be spectrum inefficient to implement the over-the-air calibration in the massive MIMO system. On the contrary, the self-calibration can be implemented at the BS; thus it is widely considered in the massive MIMO system [11, 15, 16]. A number of research activities have been developed from the perspective of the so-called relative self-calibration [15, 16], where the underlying concept is to relatively calibrate the BS antennas based on the ratio of the Tx RF response to the Rx RF response. By contrast, we proposed a calibration scheme in [17, 18], namely "inverse calibration". Here the design principles include using low-cost calibration circuits at the BS to reliably estimate the RF responses and taking into account the compound effect of the reciprocity and estimation errors. Furthermore, the work in [18] provided an analysis of the pre-equalisation performance of both inverse and relative calibration schemes by evaluating their ergodic sum rates.

One critical research gap identified in [18] is that, in order to equalise and decode the received signal, each UT should have an estimate of the effective channel gain. This channel gain is a compound of the actual channel and the calibration matrix. Hence, the post-equalisation mean-square error (MSE) at each UT is an important performance metric to evaluate the effectiveness of the calibration schemes. In this work, we aim at an in-depth analysis of the post-equalisation MSE performance of massive MIMO systems with self-calibration. More specifically, by taking into account the channel reciprocity error, imperfect CSI and the simplest precoding scheme, i.e., MRT, we derive closed-form expressions of the receive MSE for both calibration schemes. The comprehensive performance analysis in this work provides important insights for the practical system design, including that: *a)* the relative calibration suffers from the effect of estimation error amplification, which can even outweigh the benefit of calibration in certain cases, such as in the low region of the estimation signal-to-noise ratio (SNR); *b)* the inverse calibration outperforms the relative calibration, in the massive MIMO system under compound effect of both reciprocity and estimation errors.

Notation: A random variable $x \sim \mathcal{CN}(\mu, \sigma^2)$ is complex Gaussian distributed with mean μ and covariance σ^2; while $x \sim \mathcal{N}_{\mathrm{T}}(\mu, \sigma^2), x \in [a, b]$, is truncated Gaussian distributed with mean μ, variance σ^2 and truncated range $[a, b]$, where $-\infty < a < b < \infty$. Vectors and matrices are denoted by lower and upper case boldface characters, respectively. An $M \times M$ identity matrix is denoted by $\mathbf{I}_M$, and $\mathrm{diag}(\cdot)$ represents the diagonalisation operator to transform a vector to a diagonal matrix. Operators $\mathbb{E}\{\cdot\}$, $\mathrm{var}(\cdot)$, $\mathrm{tr}(\cdot)$, $(\cdot)^*$, $(\cdot)^T$ and $(\cdot)^H$ represent mathematical expectation, variance, matrix trace, complex conjugate, transpose and Hermitian transpose, respectively. The magnitude of a complex number is denoted by $|\cdot|$, while $\|\cdot\|$ is the matrix Frobenius norm. The imaginary unit is denoted by j. The exponential function is defined as $\exp(\cdot)$. Unless otherwise stated, superscript/subscript 'b' stands for BS, and 't' and 'r' correspond to Tx and Rx, while 'u' and 'd' represent UL and DL, respectively.

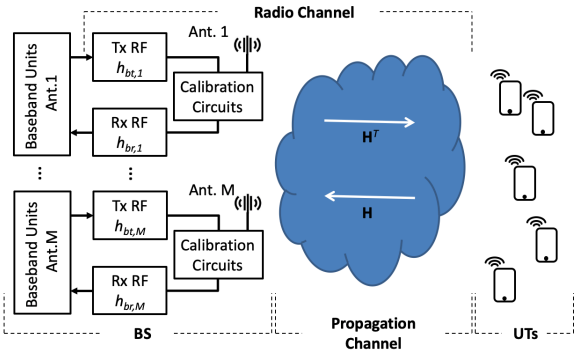

Figure 1: A TDD massive MU-MIMO System with calibration circuits.

2 SYSTEM MODEL

The considered system model is a TDD massive MU-MIMO as shown in Fig. 1, where K single-antenna UTs are served simultaneously by one BS. The BS has M antennas that connect to individual RF chains equipped with calibration circuits. The overall radio channel comprises the propagation channel as well as Tx and Rx RF frontends at the BS side. We assume $M \gg K$, and the time delay from the UL channel estimation to the DL transmission is less than the coherence time of the channel, and the impact of imperfect channel reciprocity at the single-antenna UT side on the system performance is negligible [5].

2.1 Modelling of Channel Reciprocity Error

As illustrated in Fig. 1, UL and DL propagation channels are reciprocal, whereas the Tx and Rx frontends are not [10–12]. More specifically, the UL and DL propagation channel responses are denoted by $\mathbf{H} \in \mathbb{C}^{M \times K}$ and $\mathbf{H}^T$ respectively, whose entries are assumed to be independent identically distributed (i.i.d.) complex Gaussian random variables with zero mean and unit variance, i.e., $\mathcal{CN}(0, 1)$. On the other hand, the effective hardware responses of the Rx and Tx RF frontends at the BS are denoted by two diagonal matrices $\mathbf{H}_{br}, \mathbf{H}_{bt} \in \mathbb{C}^{M \times M}$, as [12]

$$\mathbf{H}_{br} = \mathrm{diag}(h_{br,1}, \cdots, h_{br,i}, \cdots, h_{br,M}), \tag{1}$$

$$\mathbf{H}_{bt} = \mathrm{diag}(h_{bt,1}, \cdots, h_{bt,i}, \cdots, h_{bt,M}), \tag{2}$$

whose i^{th} diagonal entries $h_{br,i}$ and $h_{bt,i}$ are given by

$$h_{br,i} = A_{br,i} \exp(j\varphi_{br,i}), \tag{3}$$

$$h_{bt,i} = A_{bt,i} \exp(j\varphi_{bt,i}), \tag{4}$$

respectively. Amplitude and phase reciprocity errors, $A_{br,i}, \varphi_{br,i}$ in (3) and $A_{bt,i}, \varphi_{bt,i}$ in (4) can be modelled as independent truncated Gaussian random variables as

$$A_{br,i} \sim \mathcal{N}_{\mathrm{T}}(\alpha_{br,0}, \sigma_{br}^2), A_{br,i} \in [a_r, b_r], \tag{5}$$

$$\varphi_{br,i} \sim \mathcal{N}_{\mathrm{T}}(\theta_{br,0}, \sigma_{\varphi_r}^2), \varphi_{br,i} \in [\theta_{r,1}, \theta_{r,2}], \tag{6}$$

$$A_{bt,i} \sim \mathcal{N}_{\mathrm{T}}(\alpha_{bt,0}, \sigma_{bt}^2), A_{bt,i} \in [a_t, b_t], \tag{7}$$

$$\varphi_{bt,i} \sim \mathcal{N}_{\mathrm{T}}(\theta_{bt,0}, \sigma_{\varphi_t}^2), \varphi_{bt,i} \in [\theta_{t,1}, \theta_{t,2}], \tag{8}$$

where, without loss of generality, the statistical magnitudes of these truncated Gaussian distributed variables are assumed to be static, e.g., $\alpha_{br,0}$, σ^2_{br}, a_r and b_r of $A_{br,i}$ in (5) remain constant within the considered coherence time of the channel [15].

2.2 Imperfect CSI

The UL training protocol is based on the minimum mean-square error (MMSE) channel estimation. In particular, UTs send orthogonal UL pilots to BS, of length $\tau_u \geq K$. Then the BS calculates the MMSE estimate of the actual UL channel response $\mathbf{H}_u$ as

$$\hat{\mathbf{H}}_u = a\mathbf{H}_{br}\mathbf{H} + b\mathbf{N}_u, \tag{9}$$

where

$$a = \frac{\tau_u\rho_u}{\tau_u\rho_u + 1},\ b = \frac{\sqrt{\tau_u\rho_u}}{\tau_u\rho_u + 1}. \tag{10}$$

In addition, the noise matrix $\mathbf{N}_u \in \mathbb{C}^{M\times K}$ has i.i.d. $C\mathcal{N}(0,1)$ elements, and ρ_u denotes the expected UL transmit SNR. The BS takes $\hat{\mathbf{H}}_u^T$ as the DL channel estimate $\hat{\mathbf{H}}_d$, but the actual DL channel is $\mathbf{H}_d = \mathbf{H}^T\mathbf{H}_{bt}$. As a result,

$$\hat{\mathbf{H}}_d = a\mathbf{H}_d\mathbf{E} + b\mathbf{N}_u^T, \tag{11}$$

where $\mathbf{E} = \mathbf{H}_{bt}^{-1}\mathbf{H}_{br}$ is the channel reciprocity error. According to the property of the MMSE channel estimation, the actual DL channel matrix $\mathbf{H}_d$ can be further decomposed into a combination of DL channel estimation matrix and an independent estimation error matrix [19]. Considering the effect of the channel reciprocity error $\mathbf{E}$, we have

$$\mathbf{H}_d = (\hat{\mathbf{H}}_d + \mathbf{V})\mathbf{E}^{-1}, \tag{12}$$

where the channel estimation error matrix $\mathbf{V}$ denotes the imperfect CSI. This matrix $\mathbf{V}$ has entries modelled as $C\mathcal{N}(0, \frac{1}{\tau_u\rho_u+1})$ and is independent of $\hat{\mathbf{H}}_d$. It is reasonable to further assume the independence between $\hat{\mathbf{H}}_d$, $\mathbf{V}$, and $\mathbf{E}$ (or equivalently $\mathbf{H}_{bt}$ and $\mathbf{H}_{br}$). We can see from (12) that imperfect CSI causes an *additive* distortion, $\mathbf{V}$, while imperfect reciprocity introduces a *multiplicative* distortion, $\mathbf{E}$, in the sense that $\mathbf{E}$ is multiplied with the channel estimate $\hat{\mathbf{H}}_d$ and the estimation error $\mathbf{V}$. The compound effect of the additive estimation error and the multiplicative reciprocity error can cause a significant performance degradation of the considered precoded system without a proper calibration [12].

2.3 Downlink Precoding

The BS applies the DL precoding and form the transmit signal which is represented by a vector $\mathbf{x} \in \mathbb{C}^{M\times 1}$,

$$\mathbf{x} = \sqrt{\rho_d}\lambda\mathbf{W}\mathbf{s}, \tag{13}$$

where ρ_d denotes the average transmit power at the BS, and the vector $\mathbf{s} = [s_1, \cdots s_k, \cdots, s_K]^T \in \mathbb{C}^{K\times 1}$ denotes the transmit symbol for K UTs. We assume these independent symbols have the normalised symbol power per user, such that $\mathbb{E}\left\{|s_k|^2\right\} = 1$, for $k = 1, 2, \cdots, K$. The matrix $\mathbf{W} \in \mathbb{C}^{M\times K}$ denotes the linear precoder, with a normalisation parameter λ to satisfy the transmission power constraint at the BS:

$$\mathbb{E}\left\{\|\mathbf{x}\|^2\right\} = \mathbb{E}\left\{\|\sqrt{\rho_d}\lambda\mathbf{W}\mathbf{s}\|^2\right\} = \rho_d. \tag{14}$$

Thus, we have:

$$\lambda = \sqrt{\frac{1}{\mathbb{E}\left\{\mathrm{tr}\left(\mathbf{W}\mathbf{W}^H\right)\right\}}}. \tag{15}$$

The collective received signal vector for all K UTs can be expressed as

$$\mathbf{y} = \mathbf{H}_d\mathbf{x} + \mathbf{n} = \sqrt{\rho_d}\lambda\mathbf{H}^T\mathbf{H}_{bt}\mathbf{W}\mathbf{s} + \mathbf{n}. \tag{16}$$

Here the vector $\mathbf{n} \in \mathbb{C}^{K\times 1}$ represents the collective DL received noise, with k^{th} element $n_k \sim C\mathcal{N}(0, \sigma_k^2)$, assuming $\sigma_k^2 = 1, \forall k$. For the k^{th} UT, the received signal y_K can be given as

$$y_k = \sqrt{\rho_d}\lambda\mathbf{h}_k^T\mathbf{H}_{bt}\mathbf{w}_k s_k + \sum_{i=1, i\neq k}^{K}\sqrt{\rho_d}\lambda\mathbf{h}_k^T\mathbf{H}_{bt}\mathbf{w}_i s_i + n_k, \tag{17}$$

where the $M \times 1$ vectors $\mathbf{h}_k$ and $\mathbf{w}_k$ are the k^{th} column of $\mathbf{H}$ and $\mathbf{W}$, respectively.

2.4 Calibration

We consider a so-called *pre-precoding* calibration which has better performance compared with the calibration after precoding [18]. A pre-precoding calibration matrix $\mathbf{B} \in \mathbb{C}^{M\times M}$ is introduced to compensate for the non-reciprocity, such that

$$\hat{\mathbf{H}}_{d,CL} = a\mathbf{H}_d\mathbf{E}\mathbf{B} + b\mathbf{N}_u^T\mathbf{B}, \tag{18}$$

where $\hat{\mathbf{H}}_{d,CL}$ represents the calibrated DL channel estimate. Without considering the imperfect CSI, the minimum requirement to calibrate the BS antennas is that $\mathbf{E}\mathbf{B} = c\mathbf{I}_M$, where the non-zero scalar c does not change the direction of the precoding beamformer [20]. We can see that the calculation of $\mathbf{B}$ relies on the estimation of $\mathbf{H}_{bt}, \mathbf{H}_{br}$, which can be achieved by using the calibration circuit as presented in [17, 18]. The considered calibration circuit contains simple hardware, e.g., Tx/Rx switches and couplers, thus can be easily scaled when M goes large. More details on the calibration circuit design can be found in [17, 18].

The design of relative calibration takes into account the aforementioned requirement, i.e., $\mathbf{B}_{\text{RC}} = c\mathbf{H}_{bt}\mathbf{H}_{br}^{-1}$, where the subscript "RC" refers to the relative calibration. As discussed in [18], the results based on the this minimum requirement may not able to be held in the presence of the compound effect of reciprocity error and imperfect CSI. More specifically, it can be seen from (18) that the calibration matrix $\mathbf{B}$ may amplify the power of the channel estimation error. We name this effect "estimation error amplification", which can even outweigh the benefit of calibration in the case with a significant level of channel estimation error, such as in the low region of ρ_u. In [17, 18], we proposed the inverse calibration to compensate for the effect of the channel reciprocity error, as well as to reduce the noise power of the UL channel estimation, or equivalently reduce the estimation noise variance. In particular, the inverse calibration matrix $\mathbf{B}_{\text{IC}}$ is equivalent to the inverse of the product of $\mathbf{H}_{bt}^*$ and $\mathbf{H}_{br}$. The subscript "IC" refers to the inverse calibration. In the next section, we will provide a comprehensive performance evaluation of these two calibration schemes.

3 PERFORMANCE EVALUATION

We consider the widely-used precoding algorithm [2], i.e., MRT, to carry out the performance evaluation of two considered self

calibration schemes. In this case, the precoding matrix $\mathbf{W}$ becomes

$$\mathbf{W}_{\text{mrt}} = \hat{\mathbf{H}}_{d,CL}^{H}. \tag{19}$$

Following (15), we have λ_{mrt} representing the normalisation parameter of the MRT precoding scheme, to meet the power constraint at the BS as shown in (14). We use *mean-square error* as the performance metric to analyse the post-equalisation performance. Note that our theoretical analysis contends with the compound effects on the system performance of the additive channel estimation error and multiplicative channel reciprocity error.

In practice, each UT should perform equalisation to reliably decode the received signal y_k. This is particularly important in the case with high orders of modulation and a soft decoder. The equalisation process requires the knowledge of the DL CSI, or equivalently, the effective DL channel response which consists of the precoding vector and the channel gain. We denote the effective DL channel response by g_k, which is given by

$$g_k = \sqrt{\rho_d}\lambda \mathbf{h}_k^T \mathbf{H}_{bt} \mathbf{w}_k. \tag{20}$$

The acquisition of g_k at the UT side in the massive MIMO system can be achieved efficiently by the DL beamforming training technique [21]. We assume that the training SNR is sufficiently high to guarantee the perfect knowledge of g_k at the k^{th} UT [21]. The widely used *zero-forcing equalisation* [22] is considered in this paper, such that the k^{th} UT applies the inverse of g_k to y_k for decoding. Let $\hat{s_k}$ denote the decoded signal, we have

$$\hat{s}_k = \frac{y_k}{g_k} = s_k + \sum_{i=1, i\neq k}^{K} g_i s_i + \frac{n_k}{g_k}, \tag{21}$$

where $g_i = g_k^{-1}\sqrt{\rho_d}\lambda \mathbf{h}_k^T \mathbf{H}_{bt}\mathbf{w}_i$. Based on (21), the post-equalisation MSE at the k^{th} UT can be calculated as

$$\text{MSE}_k = \mathbb{E}\left\{|\hat{s}_k - s_k|^2\right\} \tag{22}$$

$$= \mathbb{E}\left\{\left|\sum_{i=1, i\neq k}^{K} g_i s_i\right|^2\right\} + \mathbb{E}\left\{\left|\frac{n_k}{g_k}\right|^2\right\}. \tag{23}$$

Using (19), the effective channel gain at the k^{th} UT in the MRT precoded system can be given by

$$g_{k,\text{mrt}} = \sqrt{\rho_d}\lambda_{\text{mrt}} \mathbf{h}_k^T \mathbf{H}_{bt} \mathbf{w}_{k,\text{mrt}}. \tag{24}$$

Note that $g_{k,\text{mrt}}$ contains the precoding vector $\mathbf{w}_{k,\text{mrt}}$ that is first contaminated by the compound effect of the channel reciprocity error and the estimation error, and then calibrated by either relative or inverse calibration schemes. We shall analyse the performance of these two calibration schemes in terms of the receive MSE as follows.

3.1 Inverse Calibration

In this case, the effective channel gain in (24) at the k^{th} UT can be rewritten as

$$g_{k,\text{mrt}}^{\text{IC}} = \sqrt{\rho_d}\lambda_{\text{mrt}}^{\text{IC}}\left(a\mathbf{h}_k^T\mathbf{h}_k^* + b\mathbf{h}_k^T(\mathbf{H}_{br}^*)^{-1}\mathbf{n}_{u,k}^*\right), \tag{25}$$

where $\mathbf{n}_{u,k}$ is the k^{th} column of the channel estimation noise matrix $\mathbf{N}_u$. Substituting (25) in (23), the closed-form expression of the MSE can be derived as follows:

Proposition 1. *Consider a TDD massive MU-MIMO system modelled in Section 2, where the BS applies the MRT precoder and the inverse calibration, and the UTs apply the zero-forcing equalisation. The receive MSE at the k^{th} UT is given by*

$$\text{MSE}_{k,\text{mrt}}^{\text{IC}} \approx \left(\frac{a^2 + b^2E_{\bar{2}}^r}{a^2(M+1)+b^2E_{\bar{2}}^r}\right)\left(K-1+\frac{KE_{\bar{2}}^t}{\rho_d}\right), \tag{26}$$

where the expected values of the inverse square of truncated Gaussian distributed variables, i.e. $E_{\bar{2}}^r, E_{\bar{2}}^t$, are given in [18].

Proof. See Appendix A. □

3.2 Relative Calibration

In the case that the BS applies the relative calibration, (24) can be rewritten as

$$g_{k,\text{mrt}}^{\text{RC}} = \sqrt{\rho_d}\lambda_{\text{mrt}}^{\text{RC}}\left(a\mathbf{h}_k^T\mathbf{H}_{bt}\mathbf{H}_{bt}^*\mathbf{h}_k^* + b\mathbf{h}_k^T\mathbf{H}_{bt}\mathbf{H}_{bt}^*(\mathbf{H}_{br}^*)^{-1}\mathbf{n}_{u,k}^*\right). \tag{27}$$

Then we can derive the closed-form expression of the MSE as follows:

Proposition 2. *Assume that the same conditions are held as in Proposition 1, but with the relative calibration at the BS. The post-equalisation MSE at the k^{th} UT is given by*

$$\text{MSE}_{k,\text{mrt}}^{\text{RC}} \approx \left(\frac{a^2 + b^2E_{\bar{2}}^r}{a^2((M-1)c_1+2)+b^2E_{\bar{2}}^r}\right)\left(K-1+\frac{Kc_2}{\rho_d}\right), \tag{28}$$

where $c_1 = A_t^2/E_4^t$ and $c_2 = A_t/E_4^t$. The reciprocity-error-related parameter At and the 4th non-central moment of truncated Gaussian distributed variables E_4^t are given in [12] and [18], respectively.

Proof. See Appendix A. □

It can be observed from (26) and (28) that, for both inverse and relative calibration schemes, the effect of the phase reciprocity error is eliminated thus does not affect the post-equalisation MSE. However, the relative calibration is hindered by the significant residual amplitude error, e.g., c_1 and c_2 in (28), where $c_2 < c_1 < 1$. Comparing (28) with (26), we can conclude that: 1) in low DL SNR regime, such that the noise-related component in (28), i.e., Kc_2/ρ_d, is dominant, $\text{MSE}_{k,\text{mrt}}^{\text{RC}}$ may be smaller than $\text{MSE}_{k,\text{mrt}}^{\text{IC}}$. However, in this case, both calibration schemes are not able to work properly; 2) in the case of sufficiently high DL SNR, $\text{MSE}_{k,\text{mrt}}^{\text{IC}}$ can be smaller than $\text{MSE}_{k,\text{mrt}}^{\text{IC}}$. We will verify these analytical results via Monte-Carlo simulations in the following section. In addition, we would like note that the approximate expressions in Proposition 1 and 2 are accurate in the case with the asymptotically large values of the BS antennas, which is also verified in the following section.

4 SIMULATION RESULTS

In this section, we perform Monte-Carlo simulations to corroborate the analytical results developed in Section 3, and compare the performance of the concerned two calibration schemes under different scenarios. Two reference scenarios are considered which are no calibration performed "NC" and "Perfect Channel Reciprocity" where $\sigma_{bt}^2 = \sigma_{bt}^2 = \sigma_{\varphi_t}^2 = \sigma_{\varphi_t}^2 = 0$. We also consider $M = 100$, $K = 10$, the amplitude reciprocity error with $(\alpha_{bt,0}, \sigma_{bt}^2, [a_t, b_t]) =$

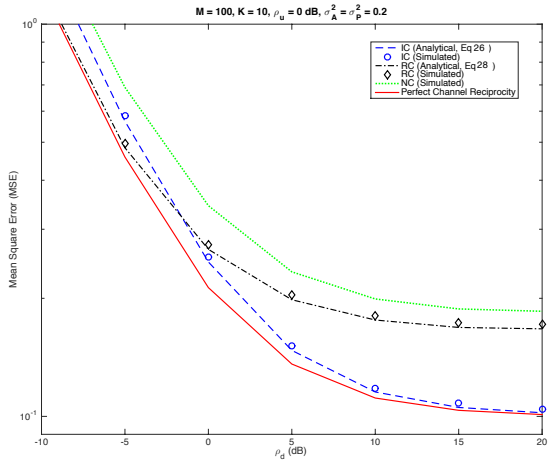

Figure 2: MSE versus DL SNR in the presence of the reciprocity error and channel estimation error with $\rho_u = 0$ dB. QPSK applied.

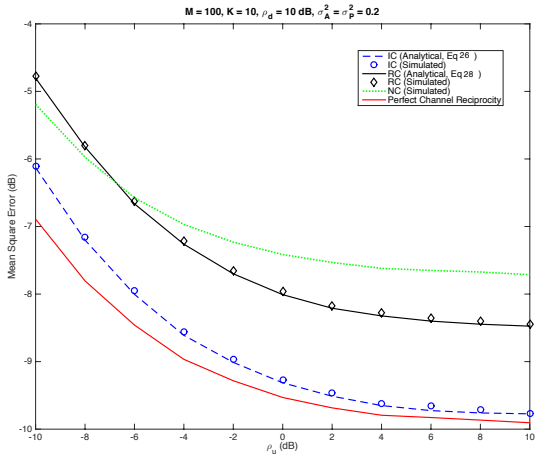

Figure 3: MSE versus UL SNR in the presence of the reciprocity error and $\rho_d = 10$ dB. QPSK applied.

$(\alpha_{br,0}, \sigma^2_{br}, [a_r, b_r]) = (0\text{ dB}, 0.2, [-4\text{ dB}, 4\text{ dB}])$, and the phase reciprocity error with $(\theta_{bt,0}, \sigma^2_{\varphi_t}, [\theta_{t,1}, \theta_{t,2}]) = (\theta_{br,0}, \sigma^2_{\varphi_r}, [\theta_{r,1}, \theta_{r,2}]) = (0^\circ, 0.2, [-50^\circ,\ 50^\circ])$. In addition, the quadrature phase shift keying (QPSK) modulation is applied at the BS, while the zero-forcing equalisation is performed at each UT as mentioned before. The orthogonal UL pilots are of length $\tau_u = K$, and the receive MSE is measured in dB.

Fig. 2 shows that the inverse calibration outperforms the relative calibration in high DL SNR regime, e.g., ρ_d from 0 dB to 20 dB. For low DL SNR, the relative calibration performs slightly better than the inverse calibration. This can be confirmed analytically by comparing (26) and (28), where $\text{MSE}^{\text{RC}}_{k,\text{mrt}}$ can be smaller than $\text{MSE}^{\text{IC}}_{k,\text{mrt}}$ when the noise-related component is dominant. However, the MSE performance of MRT is significantly affected by the noise at the UT when the DL SNR is low. For example, MSE is around -3 dB (or 50 %) when $\rho_d = -5$ dB. Therefore, it is more meaningful to consider the case with the non-trivial DL SNR, e.g., $\rho_d = 10$ dB. In this case, the performance of inverse calibration approaches to the best case scenario, whereas the performance gain of RC is negligible compared to the case without the calibration.

To verify the conclusion followed by Proposition 2, we present the MSE performance of different calibration schemes in the presence of different levels of the estimation error in Fig. 3. It is not surprised to see from Fig. 3 that the relative calibration loses its performance gain with high estimation error. On the contrary, the inverse calibration is more robust to the compound effect of the reciprocity and estimation errors.

5 CONCLUSION

In this paper, we have considered a key technical enabler in the emerging mobile networks, i.e., TDD massive MU-MIMO system. Our focus has been on the potential performance-limiting factors of such a system, which are imperfect CSI and non-reciprocity, in order to provide valuable insights into the practical system design. We have evaluated the performance of two self-calibration schemes, i.e., inverse calibration and relative calibration, in the presence of the compound effect of the multiplicative reciprocity error and the additive estimation error. The closed-formed expressions for post-equalisation MSE based on the zero-forcing equalisation of the considered system have been derived, under the assumption with the MRT precoding that affected by the compound effect of both errors. A comparative analysis based on the theoretical expressions has been provided for both calibration schemes, with the analytical results perfectly matching the simulated results in different scenarios. The paper has demonstrated that the inverse calibration in general outperforms the relative calibration, due to the fact that the former takes the compound error effect into considerations of its design principle.

ACKNOWLEDGMENTS

This work was supported by the U.K. Engineering and Physical Sciences Research Council under Grant EP/P008402/2. The authors also would like to acknowledge the support of the University of Surrey 5GIC (http://www.surrey.ac.uk/5gic) members for this work.

REFERENCES

[1] 3GPP, "NR; Physical layer; General description (Release 16)," 3rd Generation Partnership Project (3GPP), Technical Specification (TS) 38.201, Dec. 2019.
[2] T. L. Marzetta, "Noncooperative cellular wireless with unlimited numbers of base station antennas," *IEEE Trans. Wireless Commun.*, vol. 9, no. 11, pp. 3590–3600, Nov. 2010.
[3] S. Yang and L. Hanzo, "Fifty years of MIMO detection: The road to large-scale MIMOs," *IEEE Communications Surveys Tutorials*, vol. 17, no. 4, pp. 1941–1988, Sep. 2015.
[4] E. Björnson, J. Hoydis, and L. Sanguinetti, "Massive MIMO networks: Spectral, energy, and hardware efficiency," *Foundations and Trends® in Signal Processing*, vol. 11, no. 3-4, pp. 154–655, 2017.
[5] E. G. Larsson *et al.*, "Massive MIMO for next generation wireless systems," *IEEE Commun. Mag.*, vol. 52, no. 2, pp. 186–195, Feb. 2014.
[6] F. Rusek *et al.*, "Scaling up MIMO: Opportunities and challenges with very large arrays," *IEEE Signal Process. Mag.*, vol. 30, no. 1, pp. 40–60, Jan. 2013.
[7] H. Yang and T. L. Marzetta, "Performance of conjugate and zero-forcing beamforming in large-scale antenna systems," *IEEE J. Sel. Areas Commun.*, vol. 31, no. 2, pp. 172–179, Feb. 2013.
[8] D. Mi, "Massive MIMO with imperfect channel state information and practical limitations." Ph.D. dissertation, University of Surrey, June 2017. [Online]. Available: http://epubs.surrey.ac.uk/841236/

[9] J. Hoydis, S. ten Brink, and M. Debbah, "Massive MIMO in the UL/DL of cellular networks: How many antennas do we need?" *IEEE J. Sel. Areas Commun.*, vol. 31, no. 2, pp. 160–171, Feb. 2013.

[10] E. Björnson *et al.*, "Massive MIMO systems with non-ideal hardware: Energy efficiency, estimation, and capacity limits," *IEEE Trans. Inf. Theory*, vol. 60, no. 11, pp. 7112–7139, Nov. 2014.

[11] R. Rogalin *et al.*, "Scalable synchronization and reciprocity calibration for distributed multiuser MIMO," *IEEE Trans. Wireless Commun.*, vol. 13, no. 4, pp. 1815–1831, Apr. 2014.

[12] D. Mi, M. Dianati, L. Zhang, S. Muhaidat, and R. Tafazolli, "Massive MIMO performance with imperfect channel reciprocity and channel estimation error," *IEEE Trans. Commun.*, vol. 65, no. 9, pp. 3734–3749, Sept. 2017.

[13] X. Jiang *et al.*, "A framework for over-the-air reciprocity calibration for TDD massive MIMO systems," *IEEE Transactions on Wireless Communications*, vol. 17, no. 9, pp. 5975–5990, 2018.

[14] X. Luo, F. Yang, and H. Zhu, "Massive MIMO self-calibration: Optimal interconnection for full calibration," *IEEE Transactions on Vehicular Technology*, vol. 68, no. 11, pp. 10 357–10 371, 2019.

[15] C. Shepard *et al.*, "Argos: Practical many-antenna base stations," in *Proc. 18th Annu. Int. Conf. Mobile Comput. Netw.*, 2012, pp. 53–64.

[16] W. Zhang *et al.*, "Large-scale antenna systems with UL/DL hardware mismatch: Achievable rates analysis and calibration," *IEEE Trans. Commun.*, vol. 63, no. 4, pp. 1216–1229, Apr. 2015.

[17] D. Mi, L. Zhang, M. Dianati, S. Muhaidat, and P. Xiao, "A self-calibration scheme for TDD massive MIMO with imperfect channel estimation," in *IEEE Sensor Array and Multichannel Signal Processing Workshop (SAM)*, 2018, pp. 89–93.

[18] D. Mi, L. Zhang, M. Dianati, S. Muhaidat, P. Xiao, and R. Tafazolli, "Self-calibration for massive MIMO with channel reciprocity and channel estimation errors," in *IEEE Global Communications Conference (GLOBECOM)*, 2018, pp. 1–7.

[19] S. M. Kay, *Fundamentals of Statistical Signal Processing: Estimation Theory.* Upper Saddle River, NJ, USA: Prentice-Hall, Inc., 1993.

[20] T. Schenk, *RF Imperfections in High-rate Wireless Systems: Impact and Digital Compensation.* Springer Netherlands, 2008. [Online]. Available: https://books.google.co.uk/books?id=nLzk11P15IAC

[21] H. Q. Ngo, E. G. Larsson, and T. L. Marzetta, "Massive MU-MIMO downlink TDD systems with linear precoding and downlink pilots," in *2013 51st Allerton*, Oct. 2013, pp. 293–298.

[22] D. Tse and P. Viswanath, *Fundamentals of Wireless Communication.* New York, NY, USA: Cambridge University Press, 2005.

[23] Y. Lim, C. Chae, and G. Caire, "Performance analysis of massive MIMO for cell-boundary users," *IEEE Trans. Wireless Commun.*, vol. 14, no. 12, pp. 6827–6842, Dec. 2015.

[24] H. Wei, D. Wang, H. Zhu, J. Wang, S. Sun, and X. You, "Mutual coupling calibration for multiuser massive MIMO systems," *IEEE Trans. Wireless Commun.*, vol. 15, no. 1, pp. 606–619, Jan. 2016.

A PROOF OF PROPOSITION 1 AND 2

Recall (23), we notice that there are two uncorrelated terms in (23) which can be further simplified due to the property of s_i and n_k. More specifically,

$$\mathbb{E}\{|\sum_{i=1,i\neq k}^{K} g_i s_i|^2\} = \sum_{i=1,i\neq k}^{K} \mathbb{E}\left\{|g_i s_i|^2\right\} = \sum_{i=1,i\neq k}^{K} \mathbb{E}\left\{|g_i|^2\right\}, \tag{29}$$

$$\mathbb{E}\left\{\left|\frac{n_k}{g_k}\right|^2\right\} = \mathbb{E}\left\{\frac{1}{|g_k|^2}\right\}. \tag{30}$$

Thus the MSE can be calculated based on the values of $\mathbb{E}\{|g_i|^2\}$ and $\mathbb{E}\{|g_k|^{-2}\}$.

A.1 Inverse Calibration

In the case that the inverse calibration is considered at the BS, we have

$$\mathbb{E}\{\left|g^{\text{IC}}_{k,\text{mrt}}\right|^{-2}\} = \mathbb{E}\left\{\frac{1}{\left|\sqrt{\rho_d}\lambda^{\text{IC}}_{\text{mrt}}\left(a\mathbf{h}_k^T\mathbf{h}_k^* + b\mathbf{h}_k^T(\mathbf{H}_{br}^*)^{-1}\mathbf{n}_{u,k}^*\right)\right|^2}\right\} \tag{31}$$

$$= \frac{1}{\rho_d(\lambda^{\text{IC}}_{\text{mrt}})^2}\mathbb{E}\left\{\frac{1}{a^2\|\mathbf{h}_k\|^4 + b^2\left|\mathbf{h}_k^T(\mathbf{H}_{br}^*)^{-1}\mathbf{n}_{u,k}^*\right|^2}\right\}. \tag{32}$$

In order to calculate the expectation in (32), we first consider a simplified scenario without the estimation error, where the aforementioned expectation becomes $\mathbb{E}\{\|\mathbf{h}_k\|^{-4}\}$. Based on [12, Proposition 2], we have

$$\mathbb{E}\left\{\frac{1}{\|\mathbf{h}_k\|^4}\right\} = \frac{1}{\mathbb{E}\{\|\mathbf{h}_k\|^4\}} + O\left(\frac{\text{var}(\|\mathbf{h}_k\|^4)}{\mathbb{E}\{\|\mathbf{h}_k\|^4\}^3}\right). \tag{33}$$

The term $\left(\text{var}(\|\mathbf{h}_k\|^4)/\mathbb{E}\{\|\mathbf{h}_k\|^4\}^3\right)$ in (33) is a function of M, as given by [23]

$$\frac{\text{var}(\|\mathbf{h}_k\|^4)}{\mathbb{E}\{\|\mathbf{h}_k\|^4\}^3} = \frac{4M^3 + 10M^2 + 6M}{(M^2+M)^3}, \tag{34}$$

whose value is negligible when M is large. Then one can easily prove that

$$\mathbb{E}\left\{\frac{1}{\|\mathbf{h}_k\|^4}\right\} \approx \frac{1}{\mathbb{E}\{\|\mathbf{h}_k\|^4\}} = \frac{1}{M^2+M}. \tag{35}$$

The approximation in (35) tightly matches the exact value of $\mathbb{E}\{\|\mathbf{h}_k\|^{-4}\}$ when M goes large, based on Lhospital's Rule. In fact, when M goes to infinity, we have

$$\|\mathbf{h}_k\|^4 \xrightarrow{\text{a.s.}} M^2 + M. \tag{36}$$

Using the generalised results in [18], we can derive the following tight approximations for large or moderately large M:

$$|\mathbf{h}_k^T\mathbf{H}_{bt}\mathbf{H}_{bt}^*\mathbf{h}_k^*|^2 \xrightarrow{\text{a.s.}} M\left(2E_4^t + (M-1)A_t^2\right), \tag{37}$$

$$|\mathbf{h}_k^T\mathbf{H}_{bt}\mathbf{H}_{bt}^*\mathbf{h}_i^*|^2 \xrightarrow{\text{a.s.}} ME_4^t, \tag{38}$$

$$|\mathbf{h}_k^T\mathbf{H}_{br}^{-1}\mathbf{h}_i^*|^2 \xrightarrow{\text{a.s.}} ME_{\frac{1}{2}}^r, \tag{39}$$

$$|\mathbf{h}_k^T(\mathbf{H}_{bt}\mathbf{H}_{br}^*)^{-1}\mathbf{h}_i^*|^2 \xrightarrow{\text{a.s.}} ME_{\frac{1}{2}}^tE_{\frac{1}{2}}^r. \tag{40}$$

The terms $A_t, E_{\frac{1}{2}}^t, E_{\frac{1}{2}}^r$ and E_4^t can be found in [8]. Based on (36) and (39), we have

$$\mathbb{E}\left\{\left|g^{\text{IC}}_{k,\text{mrt}}\right|^{-2}\right\} \approx \frac{KE_{\frac{1}{2}}^t\left(a^2 + b^2E_{\frac{1}{2}}^r\right)}{\rho_d\left(a^2(M+1) + b^2E_{\frac{1}{2}}^r\right)}. \tag{41}$$

Consider the technique in [12, Eq. (95)] and [24, Eq. (14)], we also have

$$\mathbb{E}\left\{\left|g^{\text{IC}}_{i,\text{mrt}}\right|^2\right\} = \mathbb{E}\left\{\left|\frac{a\mathbf{h}_k^T\mathbf{h}_i^* + b\mathbf{h}_k^T(\mathbf{H}_{br}^*)^{-1}\mathbf{n}_{u,i}^*}{a\mathbf{h}_k^T\mathbf{h}_k^* + b\mathbf{h}_k^T(\mathbf{H}_{br}^*)^{-1}\mathbf{n}_{u,k}^*}\right|^2\right\} \tag{42}$$

$$\approx \frac{a^2 + b^2E_{\frac{1}{2}}^r}{a^2(M+1) + b^2E_{\frac{1}{2}}^r}. \tag{43}$$

Substituting (43) in (29), and applying the completed (29) along with (41), we arrive at (26) in Proposition 1.

A.2 Relative Calibration

Similar to that of the inverse calibration, we have

$$\mathbb{E}\left\{\left|g^{\text{RC}}_{k,\text{mrt}}\right|^{-2}\right\} \approx \frac{KA_t\left(a^2 + b^2E_{\frac{1}{2}}^r\right)}{\rho_d\left(a^2((M-1)A_t^2 + 2E_4^t) + b^2E_4^tE_{\frac{1}{2}}^r\right)}, \tag{44}$$

$$\mathbb{E}\left\{\left|g^{\text{RC}}_{i,\text{mrt}}\right|^2\right\} \approx \frac{a^2 + b^2E_{\frac{1}{2}}^r}{a^2((M-1)A_t^2 + 2E_4^t) + b^2E_4^tE_{\frac{1}{2}}^r}. \tag{45}$$

Then we can derive (28) in Proposition 2.